MARS ROVER COLOUR VISION: GENERATING THE TRUE COLOURS OF MARS

Dave Barnes

Aberystwyth University, Penglais, Aberystwyth, SY23 3DB, UK
{*dpb@aber.ac.uk*}

ABSTRACT

Mars rover colour vision typically employs multi-spectral imaging to generate natural-colour images that allow a planet to be viewed as if a human was present on the surface. As surface colour is dependent upon both surface reflectance/absorption properties and the surface illumination, getting the surface solar spectrum irradiance correct is vital for planetary colourimetry. Associated with a solar spectral power distribution (SPD) is its correlated colour temperature (CCT) which determines the reference white point for the colour image processing. If the CCT is wrong, then the white point will be wrong, and hence the colours will be wrong. New methods are being developed whereby a 'typical' Mars sol-light spectral distribution can be computed based upon the actual or desired CCT. Knowledge of the CCT allows the application of new chromatic adaptation transformations, whereby the martian surface can be viewed as if it had been illuminated by other terrestrial light sources as opposed to just Mars sol-light. The paper presents early results towards generating 'typical' Mars illuminants, and provides examples of CCT-based natural-colour image generation, and chromatic adaptation.

Key words: Natural Colour; Correlated Colour Temperature; Chromatic Adaptation.

1. INTRODUCTION

Given the previous science cameras flown to Mars, a good deal of research has been conducted in the area of processing multi-spectral image data to generate terrain Region of Interest (ROI) reflectance spectra, and colour corrected image products. The missions include the Viking Landers (VL) (1976) [10], the Mars Pathfinder (MPF) lander and the Sojourner rover (1997) [16], the Mars Exploration Rovers (MER) Spirit (2004 to 2010) and Opportunity (2004, still operational) [4], the Phoenix (PHX) lander (2008) [15], and the Mars Science Laboratory (MSL) (2012) [9]. Throughout these missions, multi-spectral image data have been captured and radiometrically and colorimetrically processed, and an important product has been the generated colour images.

As surface colour is dependent both upon surface reflectance/absorption properties, and the surface illumination, then getting the surface solar spectrum correct for Mars colourimetry is vital. The term *surface solar spectrum* is used here to refer to the solar spectral irradiance having passed through the atmosphere. Associated with a solar spectral power distribution (SPD) is its correlated colour temperature (CCT) which determines the reference white point for the colour image processing. If careful attention is not paid to using the correct solar spectrum and therefore CCT, then the white point will be wrong and hence the colours will be wrong. A common approach in Mars exploration has been to use the Air Mass Zero ($AM0$) reference solar spectral irradiance at the top of Earth's atmosphere. This is usually scaled using an inverse-square law to the average heliocentric distance of Mars, and then an attenuation estimate of the effects of dust in the atmosphere is applied. However such an approach is not without a number of drawbacks such as the highly eccentric solar orbit of Mars, and dust attenuation models based upon limited true optical depth knowledge.

An alternative approach is to take reflectance measurements of an in-situ calibration target that has been characterised and calibrated prior to launch. All of the Mars missions mentioned previously have flown a radiometric calibration target which has been accommodated on the lander or rover so that it can be imaged by the multi-spectral cameras. By sampling the radiometrically corrected data files generated after calibration target imaging, and comparing the measured calibration target regions with pre-flight data, then using a standard radiometric relationship, the surface solar spectrum can be found for various Sun angles [13]. Whilst this direct measurement of the solar spectral irradiance may offer an improvement over the $AM0$ related approach, the method is limited by the total number of available spectral point samples for each derived solar spectrum. Essentially a calibration target is imaged multi-spectrally, and hence the total spectral point sample number is limited by the number of available filters. For example each of the two NASA MER rover Pancam instruments has only eleven filters in the range 432 nm to 1009 nm.

The in-situ measured solar spectra are also very specific to the particular Sun angle and the atmospheric conditions present during image capture, and hence they can-

not be described as *typical* SPDs of Mars sol-light. In comparison to a specific in-situ measured surface solar spectrum that is 'tied' to a given imaging activity, the availability of typical Mars spectral distributions would be advantageous because they could be used in a much larger number of colorimetric processing situations, for example the comparison of natural-colour images generated from image data captured at different locations, times, and seasons.

Historically, terrestrial colourimetry faced a similar problem in that there are in effect an infinite number of possible solar illumination conditions given the number of possible locations, times of day, different seasons, and hence different weather conditions. The solution to this problem was the introduction of *standard illuminants* that allowed for objective colour comparisons, and which removed one key source of variation from calculations or the measurements of colour. Judd *et al.* [11] pioneered the work that led to the now CIE (Commission Internationale de l'Eclairage/International Commission on Illumination) standard daylight illuminants [6]. For example, $D65$ which is a typical daylight solar spectrum with a CCT $= 6504$ K.

The introduction of the CIE standard illuminants has had a profound impact upon terrestrial colourimetry. It has allowed many techniques such as natural-colour image generation, chromatic adaptation, and colour matching to be developed, and allowed practitioners to compare results irrespective of image capture locations and illumination conditions. Given such strengths then the question arises, "Could the same be done for Mars?" The paper presents early results using 50 SPDs of Mars sol-light samples that have been derived from Mars rover image data. Using these data, methods have been formulated whereby a 'typical' Mars sol-light spectral distribution can be computed based upon the desired correlated colour temperature (CCT). The paper explores the application of CCT-based Mars illuminants to natural-colour image generation. Given the knowledge of the CCT used during image processing, the paper presents results from the application of new chromatic adaptation transformations, whereby the Martian surface can be viewed as if it had been illuminated by daylight as opposed to Mars sol-light.

It should be noted that work reported here is ongoing, and the aim is to increase the current Mars SPD sample set by including data from MPF, PHX, and MSL (when NASA PDS Mastcam data are released). Thus a final SPD sample set will be several hundred in number. Because this larger sample set will cause (slight) changes to the results reported here, some items of detail (e.g. x_M and y_M equations) have been omitted from this paper. A full paper [1] will be published in the literature based upon the final Mars SPD sample set.

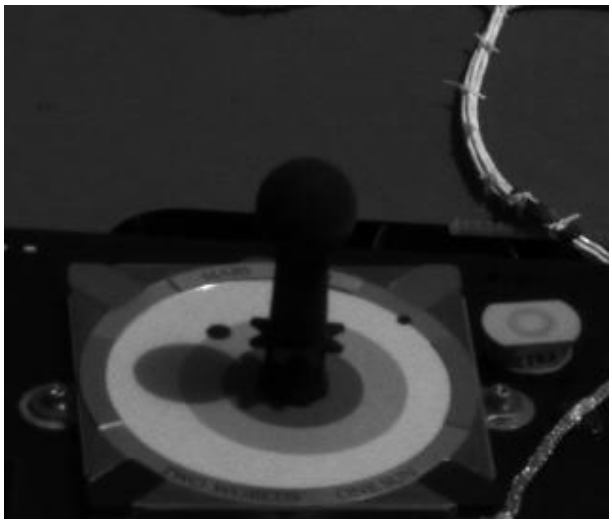

Figure 1. Radiometrically corrected (RAD) image of the MER Spirit rover calibration target captured using the Pancam instrument on sol 5*, using filter* $L5$ *with a centre wavelength of* 535 *nm.*

2. CURRENT EXPERIMENTAL DATA

Judd *et al.* [11] used a composite of 622 daylight spectral irradiance samples covering the wavelength range 330 nm to 700 nm. The composite was composed of 99 independently measured daylight samples from Ottawa Canada, 249 from Rochester USA, and 274 from Enfield UK, and thus represented daylight data measured at different locations, times of day, different seasons, and hence different weather conditions. To extend the composite data to the wavelength range of 300 nm to 830 nm, the compilation of [18] was added which contained the spectral absorptance of the Earth's atmosphere due to ozone and water vapour.

To generate an early composite of Mars sol-light spectral irradiance samples (currently 50 in number), NASA Planetary Data System (PDS) image data of the radiometric calibration targets from the Mars Exploration Rovers Spirit & Opportunity (MER) were obtained. Radiometrically corrected (RAD) files were collected for all of the filters within the range 432 nm to 1009 nm. Future work will extend the current Mars sol-light spectral irradiance samples to several hundred in number using image data from the MPF and PHX instruments, and the MSL Mastcam.

Figure 1 shows an example of the MER calibration target data downloaded from the PDS archive. The 'white', and grey regions on each calibration target were sampled (> 100 pixels) for each filter to measure the spectral radiance ($L(\lambda)$). Due to dust deposition on the calibration targets during the mission, which would cause measurement errors, the sampling was restricted to the first 50 sols (Martian days) for each rover. The amount of accumulated dust during this period was deemed to be relatively insignificant [17].

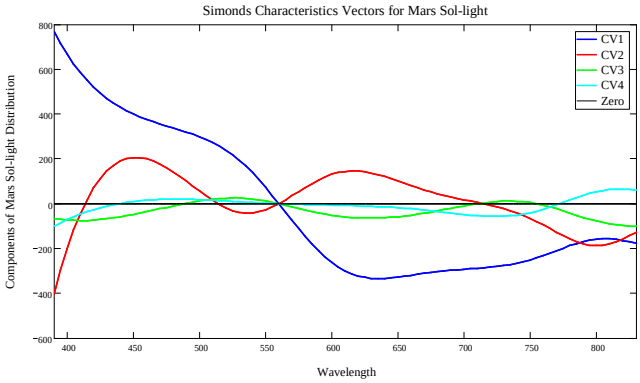

Figure 2. Graph of the first four characteristic vectors (V) derived from the composite Mars sol-light spectral distributions (currently 50 samples).

Pre-flight laboratory measured spectral reflectance $\rho(\lambda)$ data for the two targets were obtained. Using the standard radiometric relationship between spectral irradiance $E(\lambda)$, spectral radiance $L(\lambda)$, and spectral reflectance $\rho(\lambda)$ [22], the Mars solar SPDs were calculated for the two targets.

Rather than simply average the SPD data for the white and grey regions, a first-order Kalman filter was applied to 'fuse' the two data samples. This process accounted for the associated measurement variance with the resultant SPD data points each having a reduced variance and hence improved probability density function (PDF).

To complete the experimental data acquisition process, a cubic-spline was then applied to each sample. The resultant SPDs were normalised to 560 nm, and then down-sampled in increments of 5 nm to generate the composite Mars solar spectral data set. The spline-fitting, normalisation and down-sampling was undertaken to produce the data in a format that was consistent with the published CIE illuminants. Hence a direct comparison with the final generated Mars illuminants could be made.

3. MEANS AND CHARACTERISTIC VECTORS

A key technique that underpinned the work of [11] was the application of *characteristic vector analysis* to the obtained sample distributions of spectral daylight. A method adapted from [21] was used to derive the means and first four characteristic vectors using the composite of the 622 daylight samples. Simonds' characteristic vector analysis is equivalent to the method of Principal Component Analysis (PCA). The power of this approach comes from the fact that a large percentage of the variability amongst a family of daylight spectral irradiance samples may be explained by using only a few characteristic vectors.

Simonds [21] observed that any spectral irradiance curve $E(\lambda)$ can be reconstituted from the mean, $\bar{E}(\lambda)$, and characteristic vectors derived from a family of measured spectral irradiance distributions. This can be expressed by Eq. 1 where M represents a scalar multiple, $V(\lambda)$ a characteristic vector, and p is equal to the total number of characteristic vectors generated from the PCA analysis.

$$E(\lambda) = \bar{E}(\lambda) + M_1V_1(\lambda) + M_2V_2(\lambda) + M_3V_3(\lambda) + \cdots M_pV_p(\lambda)\,. \quad (1)$$

For the research reported here the non-linear iterative partial least squares (Nipals) algorithm was used to generate resultant *cumulative percentage of variance*, *Loadings* (which are equivalent to PCA eigenvectors), and *eigenvalues* (which are equivalent to Simonds' characteristic roots). The Nipals algorithm uses a different normalisation method to that used by Simonds, so to convert the resultant Loadings ($L(\lambda)$) to the equivalent of Simonds' characteristic vectors ($V(\lambda)$) a simple eigenvalue (e_{val}) scaling was performed using $V(\lambda) = L(\lambda)\,[e_{val}]^{1/2}$. The Nipals algorithm employs a mean-centered PCA approach [5].

Judd *et al.* [11] went on to use the first two characteristic vectors obtained from the set of 622 measured spectral radiant power distributions. Whilst it was reported that the use of the mean and first two characteristic vectors allowed the original distributions, "to be reconstituted remarkably well" [22], no cumulative percentage of variance results were ever published in the original paper. These results are a measure of what percentage of the original SPD set is being 'explained' by the resultant principal components. Examination of the cumulative percentage of variance results for the (currently 50) Mars composite SPD data set shows that the use of the mean and first characteristic vector alone generates a result of just 83.96%. As more characteristic vectors are added, then the cumulative percentage of variance results improve. For the two, three and four characteristic vector cases then the percentage increases to 96.71%, 98.58%, and 99.58% respectively.

4. MARS SOL-LIGHT CHROMATICITY

For a relative spectral (colour) power distribution, $\phi(\lambda)$, then using the standard CIE chromaticity equations for the *emissive* case, it is possible to calculate the XYZ tristimulus values, Eqs. 2-4. Here $\bar{x}(\lambda)$, $\bar{y}(\lambda)$, $\bar{z}(\lambda)$ are the respective colour matching functions of the 1931 CIE standard colorimetric observer [6].

$$X = \sum_{\lambda} \phi(\lambda)\bar{x}(\lambda)\Delta\lambda\,, \quad (2)$$

$$Y = \sum_{\lambda} \phi(\lambda)\bar{y}(\lambda)\Delta\lambda\,, \quad (3)$$

$$Z = \sum_{\lambda} \phi(\lambda)\bar{z}(\lambda)\Delta\lambda\,. \quad (4)$$

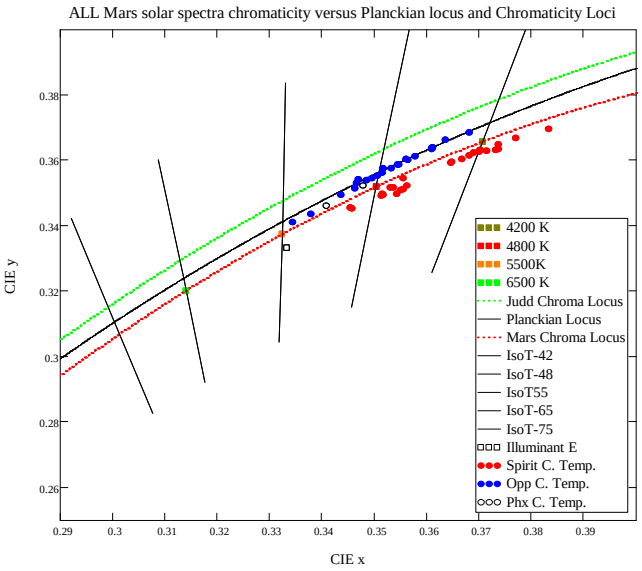

Figure 3. Chromaticities of Mars sol-light compared to the locus of chromaticities implied by the Planck radiation law. The daylight locus discovered by [11] was found to lie slightly to the 'green' side of the Planckian locus. In comparison, the Mars sol-light locus has been found to lie slightly to the 'purple' side of the Planckian locus. The straight lines intersecting the Planckian locus are examples of isotemperature lines which define loci of constant correlated colour temperature.

Substituting each derived Mars SPD for $\phi(\lambda)$, the tristimulus values were calculated for the current Mars composite SPD data set. As the fundamental colourimetric tables are the 1 nm tables in the CIE standards, a cubic-spline was applied to each SPD and the numerical summations were performed at wavelength intervals, $\Delta\lambda$, equal to 1 nm. Once the tristimulus values for each Mars SPD had been obtained, then the CIE chromaticity coordinates (x, y, and z) for each SPD were calculated by normalising the tristimulus values using Eqs. 5-7.

$$x = X/(X+Y+Z)\,, \tag{5}$$

$$y = Y/(X+Y+Z)\,, \tag{6}$$

$$z = Z/(X+Y+Z)\,. \tag{7}$$

The resultant chromaticity coordinates were then plotted on a CIE (x, y) (chromaticity) diagram, Fig. 3. This shows the chromaticities of Mars sol-light samples compared to the locus of chromaticities implied by the Planck radiation law. The Planckian locus was plotted by generating a set of blackbody radiator spectral power distributions for a range of temperatures using Planck's law, and then converting the resultant distributions to x, y chromaticity coordinates. The straight lines intersecting the Planckian locus at 4200 K, 4800 K, 5500 K, and 6500 K are examples of isotemperature lines which define loci of constant correlated colour temperature.

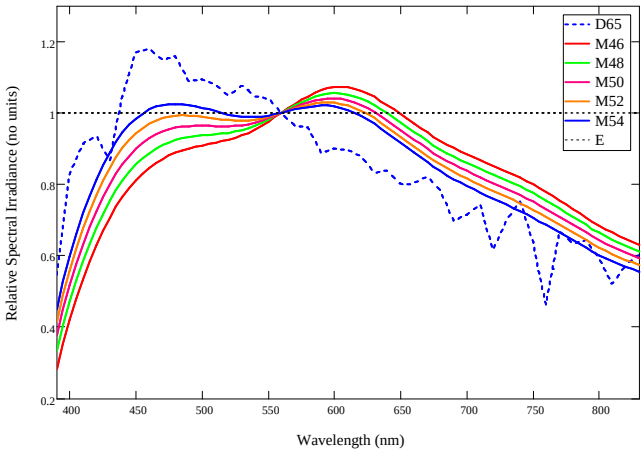

Figure 4. Relative spectral distributions of typical Mars sol-light for correlated colour temperatures: 4600 K, 4800 K, 5000 K, 5200 K, and 5400 K reconstituted from the mean and first three characteristic vectors of the composite Mars data (currently 50 samples). The spectra are normalised to 560 nm, and the CIE daylight illuminant D65, and the theoretical 'equal-energy' illuminant E are shown for comparison.

Judd *et al.* [11] applied the same process to their terrestrial spectral radiant power distributions, and discovered that the chromaticity points from the 622 samples suggested that the phases of daylight could be represented by a 'daylight locus' in the CIE chromaticity diagram. They found that this locus could be modeled by the quadratic relation $y_D = -3.000{x_D}^2 + 2.870x_D - 0.275$, where x_D, and y_D, are the daylight chromaticity coordinates. The daylight locus is shown in Fig. 3, and follows the Planckian locus but stays slightly to the (chromaticity diagram) 'green' side.

Inspection of the chromaticity points from the current 50 Mars samples has shown that the phases of Mars sol-light can be represented also by a locus. Numerical methods have been used to determine the polynomial coefficients for this Mars sol-light locus [1].

Sastri [19] observed that the proportion or absence of Rayleigh scattering in the atmosphere could affect where a daylight chromaticity point fell with respect to the Planckian locus. In an earlier paper, [20] had observed that the dust storms common in Delhi during the summer months caused daylight chromaticity points to lie on the purple side of the Planckian locus. He states, "Because of the neighboring desert, even a windy day fills the atmosphere in Delhi to some extent with fine dust, which may account for the sizeable number of points appearing on the purple side of the locus." There is significant research describing the presence of fine dust particles in the Martian atmosphere [14], therefore it is entirely appropriate that the Mars sol-light locus should be found to fall on the purple side of the Planckian locus.

The CIE determined the relationship between correlated colour temperature (T_{cp}) and x_D, thus allowing the day-

Table 1. Mars chromaticity coordinates for example CCTs based upon the current 50 *Mars SPD samples.*

Correlated colour temperature (K)	Mars chromaticity coordinates x_M	y_M
4600	0.3566	0.3564
4800	0.3505	0.3519
5000	0.3448	0.3476
5200	0.3395	0.3434
5400	0.3347	0.3393

light chromaticity coordinates (x_D and y_D) to be calculated for a specified CCT. Using the CIE equations relating T_{cp} to x_D as the baseline [6], new coefficients have been calculated for the Mars case using numerical methods to solve for a set of isotemperature line intercepts with the Mars sol-light locus. Table 1 shows the chromaticity coordinates (x_M, y_M) of typical Mars sol-light for various example values of CCT. As will be seen in section 5, values for z_M will be required and these can be obtained by exploiting the chromaticity relationship: $x_M + y_M + z_M = 1$.

5. SCALAR MULTIPLES AND CHROMATICITY COORDINATES

The significant step made by [11] was to recognise the relation between scalar multiples and CIE chromaticity coordinates. Using the CIE tristimulus value X as an example, then the irradiance specified by the distribution in Eq. 1 may by expressed as a component within Eq. 8, where $\bar{x}(\lambda)$ is one of the CIE colour matching functions defined in section 4.

$$X = \sum_{\lambda} E(\lambda)\bar{x}(\lambda)\Delta\lambda \,. \tag{8}$$

Given that the scalar multiples are constants that are independent of wavelength for any single reconstituted spectral distribution, then the tristimulus values X, Y, and Z may be written as:

$$X = X_0 + M_1X_1 + M_2X_2 + M_3X_3 + \cdots M_pX_p \,, \tag{9}$$
$$Y = Y_0 + M_1Y_1 + M_2Y_2 + M_3Y_3 + \cdots M_pY_p \,, \tag{10}$$
$$Z = Z_0 + M_1Z_1 + M_2Z_2 + M_3Z_3 + \cdots M_pZ_p \,. \tag{11}$$

Therefore the relation between scalar multiples and the CIE chromaticity coordinates x, y and z follows directly from Eqs. 9-11 given the CIE definitions for x, y, and z in Eqs. 5-7. This results in Eqs. 12-14, where $S_n = X_n + Y_n + Z_n$ and $1 \leq n \leq p$.

$$x = \frac{X_0 + M_1X_1 + M_2X_2 + M_3X_3 + \cdots M_pX_p}{S_0 + M_1S_1 + M_2S_2 + M_3S_3 + \cdots M_pS_p} \,, \tag{12}$$
$$y = \frac{Y_0 + M_1Y_1 + M_2Y_2 + M_3Y_3 + \cdots M_pY_p}{S_0 + M_1S_1 + M_2S_2 + M_3S_3 + \cdots M_pS_p} \,, \tag{13}$$
$$z = \frac{Z_0 + M_1Z_1 + M_2Z_2 + M_3Z_3 + \cdots M_pZ_p}{S_0 + M_1S_1 + M_2S_2 + M_3S_3 + \cdots M_pS_p} \,. \tag{14}$$

Given that the CIE chromaticity space is three-dimensional, then the number of (unknown) scalar multiples has to be limited to three, and hence a maximum of only three characteristic vectors can be used in the SPD reconstitution process.

For the first three characteristic vectors case, then by substituting x_M, y_M, and z_M for x, y, and z into Eqs. 12-14, and replacing X_0, X_1, ..., X_p, etc. with the coefficients a_1, a_2, ..., a_4, etc., the relationship between CCT-based chromaticity coordinates and scalar multiples can be obtained, Eqs. 15-17.

$$x_M = \frac{a_1 + a_2M_1 + a_3M_2 + a_4M_3}{d_1 + d_2M_1 + d_3M_2 + d_4M_3} \,, \tag{15}$$
$$y_M = \frac{b_1 + b_2M_1 + b_3M_2 + b_4M_3}{d_1 + d_2M_1 + d_3M_2 + d_4M_3} \,, \tag{16}$$
$$z_M = \frac{c_1 + c_2M_1 + c_3M_2 + c_4M_3}{d_1 + d_2M_1 + d_3M_2 + d_4M_3} \,. \tag{17}$$

To find the scalar multiples M_1, M_2, and M_3 required to generate a reconstituted Mars solar spectral distribution, it was necessary to solve for M_1, M_2, and M_3 from Eqs. 15-17. The details of these results will be published in [1].

6. SPECTRAL DISTRIBUTIONS OF MARS SOL-LIGHT FOR VARIOUS CORRELATED COLOUR TEMPERATURES

Having obtained the characteristic vectors for the composite Mars sol-light SPD data, and generated a solution for the scalar multiples, it was then possible to generate CCT-based Mars illuminants. Modification of Eq. 1 for the three characteristic vector case yields:

$$E_M(\lambda) = \bar{E}(\lambda) + M_1V_1(\lambda) + M_2V_2(\lambda) + M_3V_3(\lambda) \,, \tag{18}$$

where $E_M(\lambda)$ is the CCT-based Mars relative spectral solar irradiance (Mars illuminant). $\bar{E}(\lambda)$ and $V_1(\lambda)$, $V_2(\lambda)$, $V_3(\lambda)$, are the mean and first three characteristic vectors obtained from the Nipals work described in section 3. For any desired CCT (T_{cp}), the scalar multiples M_1, M_2, and M_3, can be calculated and substituted into Eq. 18.

Tab. 2 shows the obtained scalar multiples required to reconstitute spectral distribution curves of typical Mars sollight for five example values of CCT. Using these values, $E_M(\lambda)$ has been calculated for each case, and the resultant Mars illuminant spectra are shown in Fig. 4. As the CCT increases, then it can be seen that the 'blue' spectral region increases with respect to the relative irradiance, whilst the 'red' spectral region decreases. All of the Mars spectra shown have a relatively large 'hump' in the 'orange' spectral region. The CIE daylight illuminant $D65$ is shown for comparison.

7. APPLICATION OF CCT AND MARS ILLUMINANTS

Having established a method whereby Mars illuminants could be reconstructed for any given correlated colour temperature, it was then possible to explore the application of CCT and Mars illuminants to a number of areas of Mars surface science.

7.1. Generating Mars Natural-Colour Images

An important data product for all of the past surface missions to Mars has been the natural-colour images that have been generated from the measured surface reflectance spectra [10, 16, 4, 15]. The term 'natural-colour' is used here to differentiate between false-colour products whereby surface objects may be assigned artificial image pixel colours, for example to enhance the contrast between different objects during science analysis. In comparison natural-colour images seek to represent the colours of the planetary surface as if viewed by a human physically present on the planet's surface. As such, they should be a faithful and accurate representation of the colour physics for the given scene.

Using the CIE standardised method for the *reflective* (or *transmissive*) case, then for Eqs. 2-4, $\phi(\lambda) = R(\lambda)S(\lambda)$, where $R(\lambda)$ is the spectral reflectance of the object colour, and $S(\lambda)$ is the relative spectral power distribution of the illuminant. Substitution for $\phi(\lambda)$ yields Eqs. 19-21:

Table 2. Example scalar multiples based upon the current 50 *Mars SPD samples.*

Correlated colour temperature (K)	Scalar Multiples M_1	M_2	M_3
4600	0.0126	0.0031	−0.0007
4800	0.0992	0.0436	−0.0138
5000	0.1809	0.0916	−0.0303
5200	0.2583	0.1454	−0.0495
5400	0.3317	0.2037	−0.0707

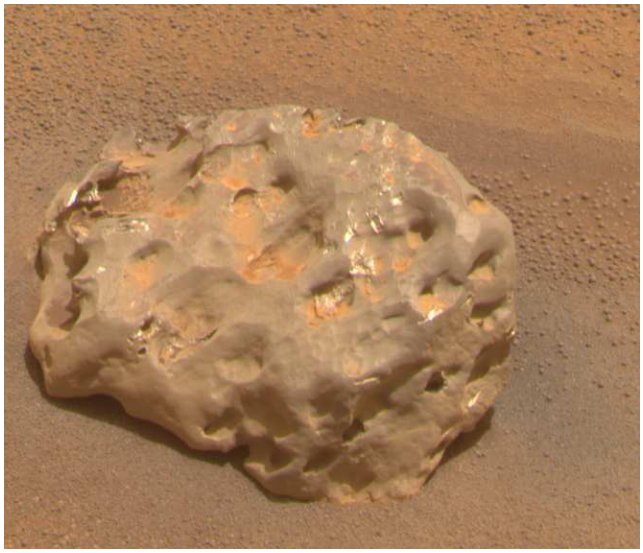

Figure 5. Example natural-colour image created using RCIPP and the generated Mars illuminant - $M54$. The data were captured by MER Opportunity on sol 346, and the image shows a discovered Mars meteorite informally named "Heat Shield Rock".

$$X = k \sum_{\lambda} R(\lambda)S(\lambda)\bar{x}(\lambda)\Delta\lambda \,, \quad (19)$$

$$Y = k \sum_{\lambda} R(\lambda)S(\lambda)\bar{y}(\lambda)\Delta\lambda \,, \quad (20)$$

$$Z = k \sum_{\lambda} R(\lambda)S(\lambda)\bar{z}(\lambda)\Delta\lambda \,, \quad (21)$$

where k is a normalisation constant and is chosen to give $Y = 100$ for the case of a perfect white Lambertian reflector, ($R(\lambda) = 1$), i.e. when an object reflects 100% for all wavelengths. Further details for generating Mars natural-colour images can be found in [3]. This describes a software-based Radiometric and Colourimetric Image Processing Pipeline (RCIPP), which has been designed and implemented by the author in Mathcad® and subsequently ported to IDL® (for inclusion into ENVI®). An enhanced version of RCIPP will be used to process image data captured by the multi-spectral Panoramic Camera (PanCam) instrument [8, 7], which is part of the science payload for the ESA/Roscosmos ExoMars 2018 mission. This mission will see a rover [2] being sent to Mars that supports many science instruments dedicated to the exploration of Mars and the search for past or present life.

Using NASA PDS image data from the MPF, MER and PHX missions, it was possible to generate natural-colour images using the RCIPP software together with the appropriate Mars illuminant. Fig. 5 shows an example of a natural-colour image produced using RCIPP and a generated Mars illuminant.

Figure 6. Example of Mars colour image chromatic adaptation. Left: The NASA MER Opportunity Pancam PDS data (sol 15) has been processed using the Mars illuminant $M48$. Middle: The left-hand ($M48$) image has been chromatically adapted to the standard CIE daylight illuminant $D65$. Right: The left-hand ($M48$) image has been chromatically adapted to the standard CIE illuminant A for a tungsten filament lamp.

7.2. Chromatic Adaptation of a Mars Illuminant

A natural spin-off from the Mars illuminant work is the ability to apply accurate chromatic adaptation to Mars image data. For example, the Mars illuminant used to generate natural-colour image data can be transformed to a standard terrestrial daylight illuminant, and hence Mars colour images can be created as if the scene had been exposed to typical daylight illumination so creating an image as it would look if the same surface region had been transported back to Earth. Given that planetary geologists base their experience upon terrestrial field trials, then presenting Mars colour image data in this way could be most informative, and provide an improved way to visualise and hence understand the Martian environment.

Eq. 22 shows that chromatic adaptation can be implemented as a linear transform of a source colour (X_S, Y_S, Z_S) into a destination colour (X_D, Y_D, Z_D) by the linear transform (M_{CA}). Knowing the source tristimulus reference white (X_{WS}, Y_{WS}, Z_{WS}) and the destination tristimulus reference white (X_{WD}, Y_{WD}, Z_{WD}), and using the Bradford chromatic adaptation transform [12] for example, then M_{CA} can be determined.

$$\begin{bmatrix} X_D \\ Y_D \\ Z_D \end{bmatrix} = [M_{CA}] \begin{bmatrix} X_S \\ Y_S \\ Z_S \end{bmatrix}. \qquad (22)$$

A set of M_{CA} transforms from $M46$, $M48$, $M50$, $M52$ and $M54$ to $D65$ have been calculated [1]. For those situations where it might be useful to see what the martian terrain would look like if imaged under typical laboratory illumination, then the transforms from $M48$ to illuminants A (tungsten filament lamp, CCT $= 2856$ K) and $F2$ (cool white fluorescent lamp, CCT $= 4230$ K) have also been calculated.

Fig. 6 shows a chromatic adaptation example. For the adaptation to illuminant $D65$ case, it can be seen that blue/grey colours have been elevated due to the raised daylight SPD in the 450 nm region, and the orange and reds have been lowered due to the decrease in daylight SPD in the 560 nm to 830 nm region. In comparison for the adaptation to illuminant A case, then the blues are minimised whilst the oranges, yellows and reds are elevated due to the increasing SPD in these wavelength regions.

8. CONCLUSIONS

The remarkably close correspondence between the CCT of a given phase of daylight and its relative SPD [22] has been the inspiration for the research reported here. The paper presents the results from only 50 SPD samples taken from the MER mission, but the work is ongoing to include SPD samples from the MPF and PHX missions, plus MSL data when these are released on the NASA PDS web site. The Mars solar SPD irradiance samples were subjected to PCA to obtain the mean and characteristic vectors (eigenvectors). Using numerical methods new formulae have been derived that allow the Mars sol-light chromaticity coordinates, x_M, and y_M to be obtained for any given correlated colour temperature (T_{cp}). Formulae to determine the scalar multiples for the three characteristic vector case have been derived which incorporate x_M, and y_M. This allows CCT-based Mars relative spectral solar irradiances (Mars illuminants) to be generated given the PCA mean and characteristic vectors obtained from the Mars solar SPD irradiance samples. Example Mars illuminants have been generated. Using the reflective case of the CIE equations for generating XYZ tristimulus values from input spectra, and selected Mars illuminants, example Mars natural-colour images have been created from the NASA PDS data archive. Transforms from a selection of Mars illuminants to the CIE standard

illuminants such as $D65$ and A were generated, and an example of the application of these transforms has been shown. Upon collection of the proposed MPF, PHX, and MSL SPD samples, then any details omitted from this paper will be published in full in the future literature [1].

ACKNOWLEDGMENTS

The research leading to these results has been funded by the UK Space Agency, Grant No. ST/G003114/1, and Grant No. ST/I002758/1, together with contributions from The European Community's Seventh Framework Programme (FP7/2007-2013), Grant Agreement No. 218814 PRoVisG, and Grant Agreement No. 241523 PRoViScout.

REFERENCES

[1] D. Barnes. Spectral distribution of typical Mars sol-light as a function of correlated colour temperature and its application to Mars colourimetry. In preparation.

[2] D. Barnes, E. Battistelli, R. Bertrand, F. Butera, et. al., and the Rover Team. The ExoMars rover and Pasteur payload Phase A study: an approach to experimental astrobiology. *International Journal of Astrobiology*, 5:221–241, 2006.

[3] D. Barnes, M. Wilding, M. Gunn, S. Pugh, L. Tyler, A. Coates, A. Griffiths, C. Cousins, N. Schmitz, A. Bauer, and G. Paar. Multi-Spectral Vision Processing for the ExoMars 2018 Mission. In *11th Symposium on Advanced Space Technologies in Robotics and Automation (ASTRA 2011)*, ESA/ESTEC, Noordwijk, The Netherlands, Apr 2011.

[4] J. Bell, D. Savransky, and M. J. Wolff. Chromaticity of the Martian sky as observed by the Mars Exploration Rover Pancam instruments. *Journal of Geophysical Research-Planets*, 111(E12), Sep. 28 2006.

[5] M. Brill. A non-PC look at principal components. *Color Research and Application*, 28(1):69–71, Feb 2003.

[6] CIE Technical Committee. *Colorimetry, Third Edition*, volume 15.3:2004. CIE Central Bureau, Vienna, Austria, 2004.

[7] C. R. Cousins, M. Gunn, B. J. Prosser, D. P. Barnes, I. A. Crawford, A. D. Griffiths, L. E. Davis, and A. J. Coates. Selecting the geology filter wavelengths for the ExoMars Panoramic Camera instrument. *Planetary and Space Science*, 71(1):80 – 100, 2012.

[8] A. D. Griffiths, A. J. Coates, R. Jaumann, H. Michaelis, G. Paar, D. Barnes, J.-L. Josset, and the PanCam Team. Context for the ESA ExoMars rover: the Panoramic Camera PanCam instrument. *International Journal of Astrobiology*, 5:269–275, 2006.

[9] J. Grotzinger, J. Crisp, A. Vasavada, R. Anderson, C. Baker, R. Barry, D. Blake, P. Conrad, K. Edgett, B. Ferdowski, R. Gellert, J. Gilbert, M. Golombek, J. Gmez-Elvira, D. Hassler, L. Jandura, M. Litvak, P. Mahaffy, J. Maki, M. Meyer, M. Malin, I. Mitrofanov, J. Simmonds, D. Vaniman, R. Welch, and R. Wiens. Mars Science Laboratory Mission and Science Investigation. *Space Science Reviews*, 170(1-4):5–56, 2012.

[10] F. O. Huck, D. J. Jobson, S. K. Park, S. D. Wall, R. E. Arvidson, W. R. Patterson, and W. D. Benton. Spectrophotometric and color estimates of the Viking lander sites. *Journal of Geophysical Research*, 82:4401–4411, Sept. 1977.

[11] D. Judd, D. MacAdam, and G. Wyszecki. Spectral Distribution of Typical Daylight as a Function of Correlated Color Temperature. *Journal of the Optical Society of America*, 54(8):1031–&, 1964.

[12] K. Lam. *Metamerism and Colour Consistency*. PhD thesis, University of Bradford, UK., 1985.

[13] G. A. Landis, D. Hyatt, and MER Athena Science Team. The solar spectrum on the Martian surface and its effect on photovoltaic performance. In *Conference Record of The 2006 IEEE 4th World Conference On Photovoltaic Energy Conversion, Vols 1 and 2*, pages 1979–1982, 2006. 4th World Conference on Photovoltaic Energy Conversion, Waikoloa, HI, May. 07-12, 2006.

[14] M. Lemmon, M. Wolff, M. Smith, R. Clancy, D. Banfield, G. Landis, A. Ghosh, P. Smith, N. Spanovich, B. Whitney, P. Whelley, R. Greeley, S. Thompson, J. Bell, and S. Squyres. Atmospheric imaging results from the Mars exploration rovers: Spirit and Opportunity. *Science*, 306(5702):1753–1756, Dec 3 2004.

[15] M. T. Lemmon, P. H. Smith, C. Shinohara, R. Tanner, P. Woida, A. Shaw, J. Hughes, R. Reynolds, R. Woida, J. Penegor, C. Oquest, S. F. Hviid, M. B. Madsen, M. Olsen, K. Leer, L. Drube, R. V. Morris, and D. T. Britt. The Phoenix Surface Stereo Imager (SSI) Investigation. In *Lunar and Planetary Institute Science Conference Abstracts*, volume 39 of *Lunar and Planetary Inst. Technical Report*, pages 2156–+, Mar. 2008.

[16] J. Maki, J. Lorre, P. Smith, R. Brandt, and D. Steinwand. The color of Mars: Spectrophotometric measurements at the Pathfinder landing site. *Journal of Geophysical Research-Planets*, 104(E4):8781–8794, Apr. 25 1999.

[17] J. Merrison. personal communication, Feb 2012.

[18] P. Moon. Proposed standard solar-radiation curves for engineering use. *Journal of the Franklin Institute*, 230:583–617, 1940.

[19] V. Sastri. Locus of Daylight Chromaticities in Relation to Atmospheric Conditions. *Journal of Physics D: Applied Physics*, 9(1):L1–L3, 1976.

[20] V. Sastri and S. Das. Spectral Distribution and Color of North Sky at Delhi. *Journal of the Optical Society of America*, 56(6):829–&, 1966.

[21] J. Simonds. Application of Characteristic Vector Analysis to Photographic and Optical Response Data. *Journal of the Optical Society of America*, 53(8):968–&, 1963.

[22] G. Wyszecki and W. S. Stiles. *Color Science: Concepts and Methods, Quantitative Data and Formulae*. John Wiley & Sons, Inc., 2nd edition, 1982.